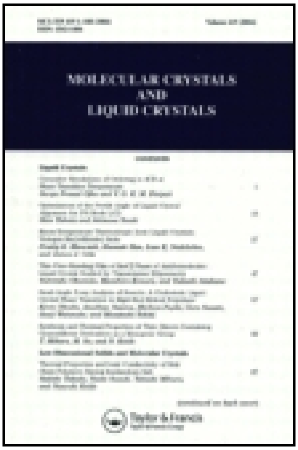

Molecular Crystals and Liquid Crystals

Publication details, including instructions for authors and subscription information:
http://www.tandfonline.com/loi/gmcl20

# Metastability of Multi-Lamellar Vesicles in a Nonionic System

Luigi Filippelli [a], Bruno Medronho [b c], Cesare Oliviero Rossi [a], Maria G. Miguel [b] & Ulf Olsson [c]

[a] Department of Chemistry, University of Calabria, Via P. Bucci, Cubo, Arcavacata, Italy

[b] Department of Chemistry, University of Coimbra, Coimbra, Portugal

[c] Physical Chemistry 1, Center of Chemistry and Chemical Engineering, Lund University, Lund, Sweden

Version of record first published: 18 Mar 2009

To cite this article: Luigi Filippelli, Bruno Medronho, Cesare Oliviero Rossi, Maria G. Miguel & Ulf Olsson (2009): Metastability of Multi-Lamellar Vesicles in a Nonionic System, Molecular Crystals and Liquid Crystals, 500:1, 166-181

To link to this article: http://dx.doi.org/10.1080/15421400802714114

*Mol. Cryst. Liq. Cryst.*, Vol. 500, pp. 166–181, 2009
Copyright © Taylor & Francis Group, LLC
ISSN: 1542-1406 print/1563-5287 online
DOI: 10.1080/15421400802714114

# Metastability of Multi-Lamellar Vesicles in a Nonionic System

**Luigi Filippelli[1], Bruno Medronho[2,3], Cesare Oliviero Rossi[1], Maria G. Miguel[2], and Ulf Olsson[3]**
[1]Department of Chemistry, University of Calabria, Via P. Bucci, Cubo, Arcavacata, Italy
[2]Department of Chemistry, University of Coimbra, Coimbra, Portugal
[3]Physical Chemistry 1, Center of Chemistry and Chemical Engineering, Lund University, Lund, Sweden

*Nuclear magnetic resonance spectroscopy and rheological analysis have been used to investigate the stability of mechanically induced tri-ethylene-glycol-mono-n-decyl-ether ($C_{10}E_3$)/deuterium oxide ($D_2O$) multi-lamellar vesicles (MLVs) and the transition from MLVs to planar lamellae. It was found that MLVs prepared by vortex stirring, relax back to the lamellar phase in a few hours while the relaxation of the shear induced MLVs takes days. Pulsed gradient spin echo and water self-diffusion coefficient experiments, revealed that the MLVs texture, obtained by vortex stirring, is composed of large size structures. These data indicate that the kinetics of lamellar re-formation depend on the MLVs number density.*

**Keywords:** $C_{10}E_3$, lamellar phase; MLVs; relaxation time; rheo-NMR

## INTRODUCTION

In recent years there has been a considerable interest in the study of the classical lamellar phase which can be seen as a 1D stack of 2D liquid domains of planar sheets. More interestingly is the fact that manifold structural changes in the mesoscopic order can be achieved by shear flow. For instance, changes in layer orientation have been extensively reported [1–7] Theoretical work has also been done and able to simulate some of the practical observations in the shear induced layer orientation transition [8,9]. Of special interest are systems

Address correspondence to Cesare Oliviero Rossi, Department of Chemistry, University of Calabria, Via P. Bucci, Cubo 14/D, Arcavacata 87036, Italy. E-mail: cesare.oliviero@unical.it

where the bilayer sheets fold to form closed structures such as multilamellar vesicles (MLVs). This is a different stationary state, induced by shear, which is separated by an out-of-equilibrium transition (planar layers to MLVs) resulting from hydrodynamical instabilities within the lamellae [10–24]. Thus, surfactant lamellar phases are often complicated by the formation of shear induced MLVs which can be originated simply by shaking the sample. The mechanism governing this transformation is still not fully understood and such complex process seems to depend on the applied shear stress and/or shear strain [25,26]. The steady states adopted by the system under flow, can be located on the so-called "shear diagram". The stability regions of MLVs and planar layers are often represented as a function of shear rate and temperature. The shear diagram of the system $C_{10}E_3/D_2O$ at 40% w/w was already reported in literature [27]. Some authors proposed that the shear induced formation of MLVs is a consequence of a mechanical flow instability of the planar lamellae at higher shear rates [28,29]. Other authors proposed that shear induced transformations are also dependent on the density of structural defects, like dislocations, in the lamellae [30–33]. When MLVs are formed, the interlamellar spacing is conserved and since MLVs fill virtually all the volume this would mean that for a spherical shape, the MLVs cannot be monodisperse. However, MLVs formed under shear flow often have a narrow size distribution which can be tuned from a few to tenths of micrometers, depending on the applied shear rate (the size scales approximately with the inverse of the square root of the shear rate). The MLVs structure is thermodynamically unstable and it persists since the transition to a lamellar phase *polydomain* occurs slowly. Hence, it relaxes back gradually, taking from few hours to several months, depending on the system and composition. The rate of the attainment of the equilibrium is a kinetic problem. In this work, the $C_{10}E_3/D_2O$ system at a surfactant concentration of 40% w/w was investigated and, for the first time, a dynamic NMR spectroscopy characterization and a rheology analysis of the MLVs-lamellar phase transition is reported. Different MLV formation procedures (vortex stirring or fixed shear rate in a rheo-couette) were used in order to understand how they affect the reformation rate of the equilibrium structure. We will demonstrate that deuterium NMR is a powerful tool for the study of shear-induced changes in lyotropic lamellar systems since the formation of vesicles has a dramatic effect on the NMR line shape. Furthermore, it is known from the investigation of phase diagrams of surfactant solutions that the deuterium NMR spectra of water as a solvent are sensitive to a coexistence of structures.

# EXPERIMENTAL PART

## Materials

Tri-ethyleneglycol mono n-decyl ether; abbreviated as $C_{10}E_3$, was purchased from Nikko Chemical Co. (Tokyo, Japan). Heavy water ($D_2O$) was purchased from Sigma Chemicals (Steinheim, Germany). Both materials have purity better than 99.8% and were used without further purification.

### *Sample Preparation*

Samples containing 40% w/w surfactant were prepared by weighing the desired amounts of surfactant and water into vials, mixing them in a vortex mixer and centrifuging them in order to remove air bubbles. All samples were prepared with $D_2O$ as a probe for deuterium NMR spectroscopy. In order to perform both NMR and rheological experiments the sample was loaded at 25°C in the Rheo or Rheo-NMR couette giving, essentially, a *powder* lamellar phase. Then, the temperature was increased to 42°C and the sample was sheared at $10 s^{-1}$ for 1 h. At this temperature and shear rate, a preferred orientation is achieved where the 1D stack of 2D fluid layers ($L_\alpha$ phase) is orientated by the flow with the bilayer normal (director) parallel to the velocity gradient [34]. After reaching the steady state, the shear was stopped and the sample was cooled down to the required temperature, retaining the orientated lamellar state. When the new temperature equilibrated, the sample was sheared at a given fixed shear rate (10 or $75 s^{-1}$) for 30 minutes. Alternatively, the sample was previously stirred in a vortex (ASAL, Italy) at $1 s^{-1}$ 10 minutes and immediately transferred to the NMR where $^2$H-NMR and PGSE self diffusion measurements were performed.

### *$^2$H-NMR*

A Bruker Avance 300 was used to record deuterium NMR spectra at 46.043 MHz. Temperature control was achieved with a Bruker Variable Temperature Unit B-VT 1000 with a sensitivity of ±0.1°C. $^2$H-NMR spectra were acquired using a quadrupole echo sequence [35]. The 90° pulse was 9 μsec, and time delays of 100 μsec were utilized in the echo sequence. Typically the number of averaged transients was from 32 to 64. Considering the abundance of the deuterium nuclei in the samples, the number was sufficient to obtain adequate signal to noise ratio. A homemade cylindrical couette cell (Rheo-NMR couette) was used to shear the sample. The inner radius of the cylinder is 3.5 mm with a gap of 1 mm. Such a rheological cell is located in a way that it fits within the RF coils of a deuterium NMR probe. This deformational flow device driven by a shaft is turned by a stepper-motor gearbox assembly mounted above the magnet bore. The basic theory of $^2$H-NMR, for liquid crystalline phase has been described elsewhere [36–40]. In anisotropic media such as randomly oriented lamellar mesophases, the quadrupole interaction of the $^2$H nucleus with its surrounding electric field gradient, give rise to spectral "powder patterns" due to the superposition of multiple spectral components, each given by the following expression

$$\Delta\nu = \frac{3}{2}\nu_Q\left(\frac{3\cos^2\theta - 1}{2}\right)\cdot S \tag{1}$$

where $\nu_Q$ is the quadrupolar coupling constant for the X-D bond and $\theta$ is the angle formed by a given micro-domain director axis and the static magnetic field. In our samples, there is a random or spherical distribution of the director axes so all values of $\theta$ contribute to the spectrum. $S$ is an order parameter describing the ordering of the O-D bonds in $D_2O$, with respect to the director of each microdomain. From the powder spectrum, the spectral separation between the 90° singularities ($\theta = 90$), defined as the quadrupole splitting $\Delta\nu$ in the following expression, can be measured:

$$\Delta\nu = \frac{3}{4}\nu_Q S \tag{2}$$

The value of the quadrupole splitting can be used to differentiate between liquid crystalline phases. Furthermore, the value of the order parameter S is time averaged. Hence, when some dynamical process occurs and if the timescale is shorter then $1/\Delta\nu$, the quadrupolar splitting decreases and the spectrum profile will turn into a very broad single peak. For our purposes, the spectrum profile gives the information we are looking for because the spectral powder pattern of the planar lamellae turns into a broad single peak when the samples are shaken or sheared. The translational diffusion in lamellar phases is highly anisotropic and restricted mainly to a given layer. Thus, for large multilamellar vesicles a distribution of averaged quadrupole couplings is expected: while diffusion in the inner shells leads to isotropic averaging, diffusion in the outer shells covers only part of the sphere so that a residual coupling results. Thus, the result is a superposition of spectra with different couplings yielding the observed relatively broad, but featureless, lines [41,42].

## PGSE-NMR

$^1$H-NMR PGSE experiments were also performed on a Bruker 300 MHz spectrometer. The spin-echo attenuations of water were measured at 25°C as a function of the time by Fourier Transform PGSE technique described by Stilbs [43]. We used the following experimental conditions: $\delta$ was varied from 1 to 70 ms while $\Delta$ and g were kept constant at 140 ms and 0.50 T/m, respectively. In a PGSE NMR experiment, the mean square displacement of the diffusing entity in a given direction, during the observed time $\Delta$, is measured by the attenuation of the spin-echo intensity and is given by the relation:

$$d = (6D\Delta)^{1/2} \tag{3}$$

where D is the self-diffusion coefficient. In neat water at room temperature, D is about $3 \cdot 10^{-9}\,m^2/s$ and is consistent with a mean square displacement of 20 μm.

For molecules undergoing an unrestricted motion, i.e. with a free three-dimensional displacement, 3d, the spin-echo attenuation on a PGSE experiment is given by [44]:

$$R_{3d} = \exp\left[-(\gamma\delta g)^2 D\left(\Delta - \frac{\delta}{3}\right)\right] = \exp[-K\,D] \tag{4}$$

where $K = (\gamma\delta g)^2\,(\Delta - \delta/3)$, $\gamma$ is the proton gyromagnetic ratio, g is the magnetic field gradient strength, $\delta$ is the width of the gradient pulses and $\Delta$ is the time occurring from the start of one pulse to the start of the next gradient pulse. When water molecules are trapped between randomly (large) oriented bilayers, which are not separated more than $10^3$ Å they diffuse in only two dimensions, 2d. Therefore, Eq. (4) was modified as [45,46]:

$$R_{2d} = \frac{\sqrt{\pi}}{2}\exp(-KD)\frac{\operatorname{erf}\left[i(KD)^{1/2}\right]}{\left[i(KD)^{1/2}\right]} \tag{5}$$

where erf is the *error* function and *i* the imaginary unity. An analogous relation was also derived for a one-dimensional diffusion. Eqs. (4) and (5) can be plotted in a diagram *ln* R *versus* KD providing a signature of the actual diffusion conditions (inserts in Fig. 6). Thus, the existence of an “ideal” lamellar mesophase can be recognized provided that the observed spin-echo attenuation shape for entrapped water follows Eq. (5). It has been reported that deviations from the theoretical 2d trends for an “ideal” lamellar phase have been interpreted as a consequence of defects in the structure. A transition from 2d to 3d behavior was analyzed in terms of bilayer sheets with water-filled defects (holes or pores) [47].

### Rheological Measurements

The rheology experiments were performed on a Physica UDS 200 rheometer using the cylindrical geometry Z3 DIN, (gap between the inner and outer cylinder of 1 mm). The instrument is equipped with a temperature control unit that was calibrated to give a temperature in the sample chamber within 0.1°C of the set value. A solvent trap was used to prevent water evaporation. The small-amplitude dynamic tests provided information on the linear viscoelastic behavior of materials through the determination of the complex shear modulus [48]:

$$\mathrm{G}^{*}(\omega) = G'(\omega) + iG''(\omega), \tag{6}$$

where $\mathrm{G}'(\omega)$ is a measure of the reversible elastic energy, while $\mathrm{G}''(\omega)$ represents the irreversible viscous dissipation of the mechanical energy.

## RESULTS AND DISCUSSION

### $^2$H-NMR Analysis

It is worthy pointing that the handling of mixture must be done carefully, in fact gently shaking of the sample produces an increase in the bluish character due to formation of bigger structures (large MLVs). The vortex shaking (stirring) effect was compared to the one produced by different shear rates ($10\mathrm{s}^{-1}$ and $75\mathrm{s}^{-1}$) at 25°C. The relaxation kinetics, of the mechanically induced MLVs texture, were initially followed by $^2$H-NMR spectroscopy. Figure 1 shows the $^2$H-NMR spectrum of the sample at 25°C (equilibrium structure) after gently loading the rheo-couette. It represents the reference spectrum for the structural analysis and is, essentially, a powder pattern (polycrystalline lamellae). Note that there were no pre-shear effects except the ones described in the sample preparation section. Figure 2 shows the time evolution of the $^2$H-NMR spectra at 25°C, performed on vortex stirred sample. The first spectrum ($\mathrm{t} = 0\mathrm{s}$) was recorded immediately after the vortex procedure and a relatively broad singlet can be observed indicating the highly curved structures. Changes in $^2$H-NMR line shape occur in time evidencing the structural relaxation towards the classical lamellar phase. The powder pattern profile is gradually formed and after 380 minutes the classical lamellar phase is recovered with a line shape similar to the one presented in Figure 1.

Figures 3 and 4 show the $^2$H-NMR spectra time evolution for the sample sheared at $10\mathrm{s}^{-1}$ and $75\mathrm{s}^{-1}$, respectively. In both cases, the initial spectrum is narrower than the one recorded for the vortex stirred sample (Fig. 3, $\mathrm{t} = 0\mathrm{s}$). Although there is not a quantitative

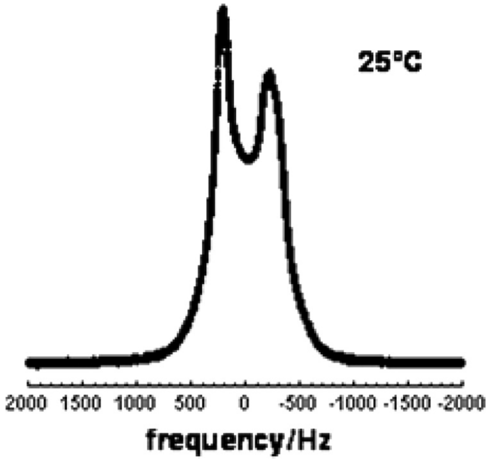

**FIGURE 1** $^2$H NMR spectrum for the sample composition of 40% w/w surfactant representing the equilibrium structure at 25°C.

relation between spectrum line width and MLVs size, it is known that the line width is proportional to the MLVs size [49] which would indicate large MLVs with the stirring procedure. The shear induced MLVs at 10 and $75\text{s}^{-1}$ show a rather low structural relaxation. The quadrupolar doublet is not recovered even after a long observation time. More important, the shear rate influence is evident; even thought the samples did not reach the equilibrium structure within the experimental time, it is clear that the sample sheared at lower shear rate ($10\text{s}^{-1}$) relax faster than the one sheared at a higher shear rate ($75\text{s}^{-1}$). The same trend was found at 35°C (data not shown). The $^2$H-NMR line shapes of the MLVs to planar lamellar relaxation in Figures 3 and 4 suggest a discontinuous process with coexistence region of both structures. It seems that when one moves towards the thermodynamic equilibrium structure (i.e., which would prevail at that temperature under zero shear), the dicontinuous/biphasic behaviour is seen, akin to a first order phase transition. The data thus suggest that the structural relaxation occurs, but is different for the three different cases and it depends crucially on the initial procedure to form the MLVs. In the case of the stirring treatment, MLVs relax faster and the polycrystalline lamellae are fully recovered after 380 min. When a constant shear rate of $10\text{s}^{-1}$ was applied to the sample, the structural relaxation was found to be considerably slower. The recorded deuterium spectra of $^2H_2O$ showed that the re-formation of the lamellar structure only started, approximately, 6 h after stopping the shear rate. It was not

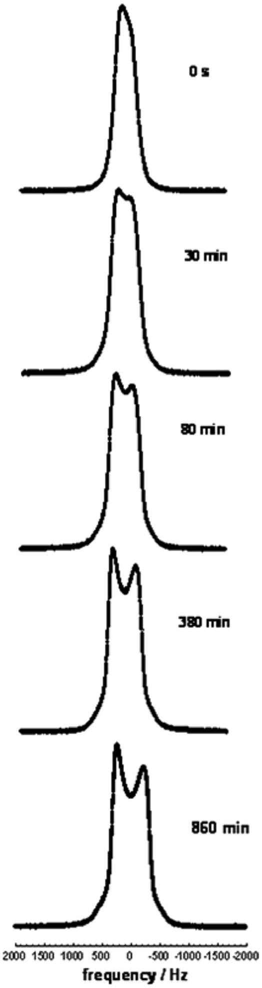

**FIGURE 2** $^{2}$H NMR spectra sequence (t = 0, 30, 80, 380, and 860 min) for the sample composition of 40% w/w surfactant previously treated by vortex stirring at 25°C.

possible to observe the complete recover of the planar $L_{\alpha}$ phase because the home made sample holder is unable to avoid water losses for long observation time. In the last case, when a higher shear rate was applied ($75s^{-1}$), it was almost imperceptible the initial reformation of powder lamellar structure. After almost 2 days, two small "shoulders" appear at each side of the singlet. A reasonable explanation for the differences observed between the systems is related to

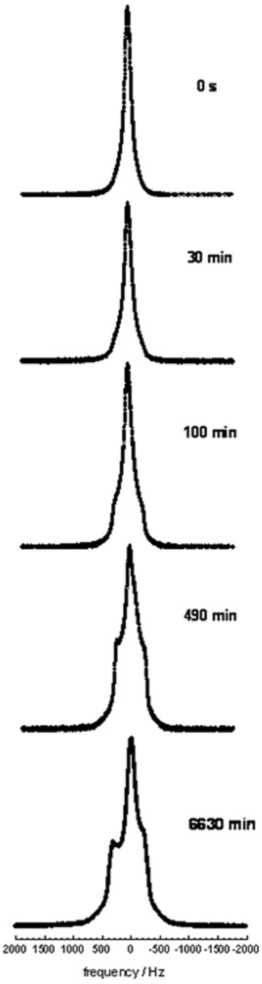

**FIGURE 3** $^2$H NMR spectra sequence ($t = 0$, 30, 100, 490, and 6630 min) for the sample composition of 40% w/w surfactant previously sheared at $10s^{-1}$ and 25°C before starting the $^2$H NMR experiments (see the experimental section for details).

polydispersity. The MLVs formed by vortex stirring are, most probably, very polydisperse with different shapes and curvatures. Theoretical studies, done by Ramos et al., argue about the possibility of having equilibrium "onions" arranged in a polydispersed array as the "Apollonian packing" [22] where small MLVs fill the free space between big MLVs. Most likely, the vortex shaking does not produce

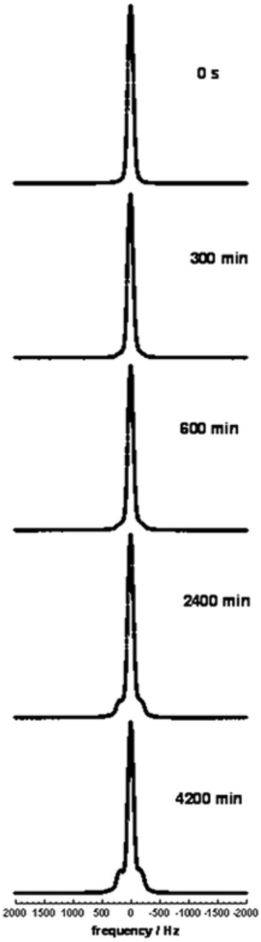

**FIGURE 4** $^2$H NMR spectra sequence (t = 0, 300, 600, 2400, and 4200 min) for the sample composition of 40% w/w surfactant previously sheared at 75s$^{-1}$ and 25°C before starting the $^2$H NMR experiments (see the experimental section for details).

a perfect "Apollonian packing", but the observed fast relaxation gives indication of something even less organized and unstable. The fact that shear induced MLVs have a narrow size distribution and are often considered to be monodisperse has a great impact in the structure stability and relaxation kinetics mainly because a balance between the viscous and elastic forces is reached turning difficult the relaxation and trapping this matastable structure. The MLVs formed at higher shear rate are smaller than the ones formed at the lower shear rate as demonstrated by the deuterium narrower lines. For higher surfactant concentrations the inter-bilayer spacing is independent on the MLV size, hence a decrease in the MLVs size is accompanied by an increase in the MLV number density, N/V, where N is the number of vesicles and V the total volume. As a practical consequence the number of "neighbors" per each MLV increases, stabilizing each MLV due to a higher cohesive energy. This cohesive energy is related to the number of contact point between objects and responsible for their higher or lower stability and has been seen in other systems like concentrated emulsions. The week gel model introduces the parameter "coordination number" which is related to the number of contact points and is another approach to explain the increase of stability of MLVs when their number density becomes higher.

### Rheology Analysis

The stability of MLVs sheared at 10 and $75^{-1}$ at 25°C was followed by the time evolution of the elastic modulus, $G'$. After the sample loading procedure and the lamellae alignment (described in the experimental section), MLVs were formed at a constant shear rate of $10s^{-1}$ for 1 h at 25°C. Then, $G'$, at a constant frequency (1 Hz) and stress (1 Pa), was recorded every 15 min up to two days (2880 min). The same procedure was applied for shear induced MLVs at $75s^{-1}$. The results for both shear rates are displayed in Figure 5. The higher elasticity of the system pre-sheared at a higher shear rate is in agreement with previous results and, essentially, is related to MLVs number density. $G'$ time evolution reflects a kind of nucleation and growth mechanism where a highly polycrystalline and defected lamellar phase is formed from the "rupture" of onions and the process occurs faster for the system pre-sheared at $10s^{-1}$ rather than for the system sheared at $75s^{-1}$. In fact, the system pre-sheared at $10s^{-1}$ shows a continuous gradual change in $G'$ from the very beginning of the experiment which is in agreement with the $^2$H-NMR line shape evolution in Figure 3. On the other hand, the system pre-sheared at $75s^{-1}$ shows no significant change in the elastic modulus during the initial 1600 minutes in agreement with the spectra evolution in Figure 4 where no major changes in the deuterium line shape are perceptible during the same period of time. The slow increase in $G'$ in the system pre-sheared at $75s^{-1}$ reflects the difficulty of obtaining the thermodynamic stable structure. Interestingly, the lamellae reformed from the MLV relaxation (in both cases), has a higher elasticity than the MLVs texture which also indicates that the lamellae structure is polycrystalline

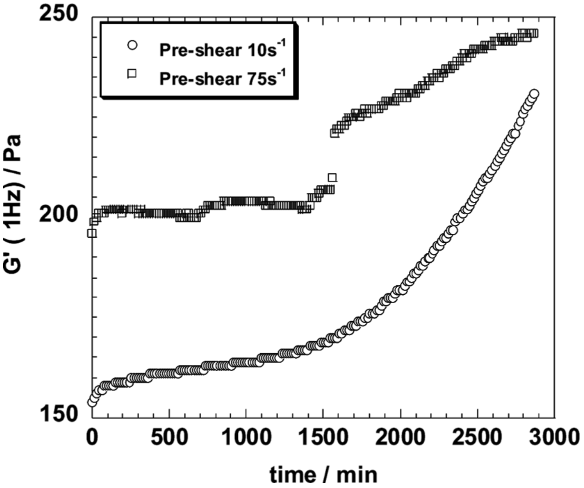

**FIGURE 5** G′ at constant frequency (1 Hz) and stress (1 Pa) evolution in time for MLVs pre-formed at $10s^{-1}$ and $75s^{-1}$ at 25°C. The elastic modulus was measured every 15 min up to 2880 min.

(powder pattern) with no preferred orientation and with high structural defect density.

### Self Diffusion Measurements

The MLVs relaxation was also investigated by water self diffusion measurements. However, due to the technical impossibility of performing self diffusion measurements under shear we were only able to perform measurements on MLVs prepared by vortex stirring (procedure described in the experimental section). This experiment was just an extra way to monitor the MLVs relaxation to lamellae by following the water molecules motion. In figure 6 the water self-diffusion coefficients versus time at 25°C are reported and three regions can be distinguished. The diffusion of water molecules confined into spherical structures, i.e. MLVs, is surely more restricted with respect to the diffusion of water into 2D “infinite” plane, i.e. classical lamellae. Thus, the linear increase of the water self diffusion in all regions indicates the formation of lamellar sheets and suggests again the nucleation and growth mechanism.

The low initial slope in region 1 can be ascribed to the high energy barrier associated to the transition MLVs-lamellae. The low slope in the region 3 can be related to a sort of saturation due to the decrease in the number density of MLVs. A reasonable agreement is found with

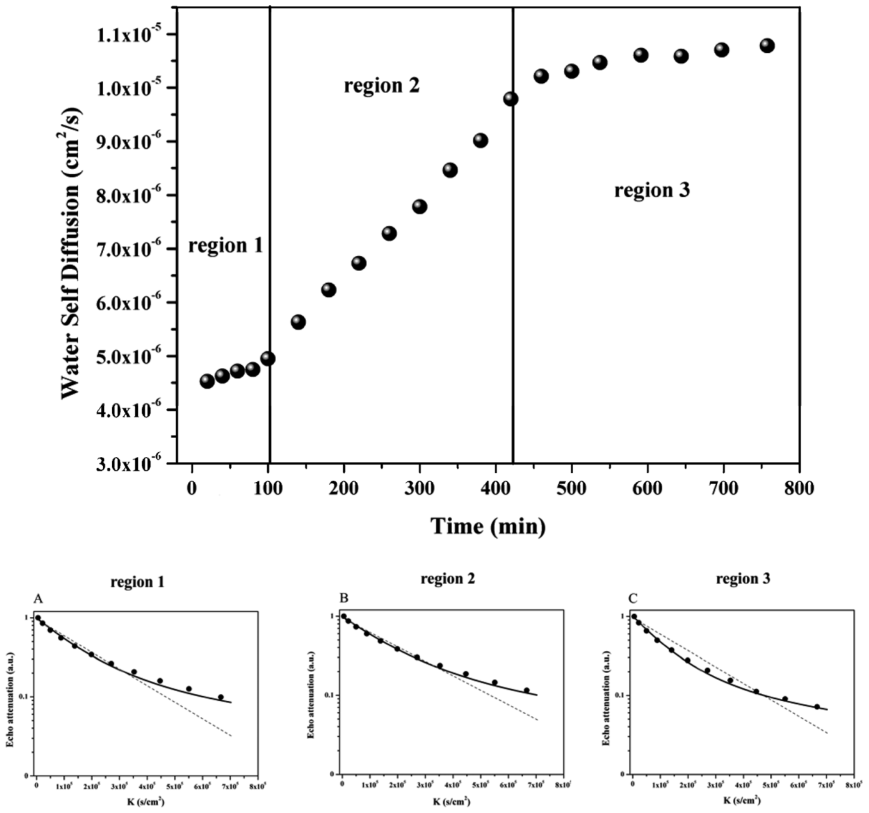

**FIGURE 6** Self-Diffusion in the 40% w/w $C_{10}E_3$ sample as a function of time after manually shaking of the sample. Inserted below are the echo attenuation plots of the 3 regions identified. The calculated best fits for the 3 d (dashed line) and 2 d (solid line) diffusion models are represented using Eqs. (4) and (5), respectively.

the $^2$H-NMR data in Figure 2 where the major changes in the deuterium line shapes occur in the first 400 min. Afterwards, the powder spectrum remains, essentially, unaffected indicating that the equilibrium structure was reached. Inserted in Figure 6 are the results of spin echo attenuation data from PGSE experiments performed at 25°C with the diffusive observation time, $\Delta$, fixed at 140 ms. The water echo attenuation decay, as a function of K. The continuous line represents the fitting of the experimental data using Eq. (5) while the dashed line represents the fitting using Eq. (4). Spin-echo attenuation plots exhibit a marked curvature reflecting a two-dimensional diffusion of water. The analysis of these PGSE-NMR experiments is in good agreement with deuterium line shapes. Moreover, Eq. (5) (derived for randomly oriented arrays of lamellar elements each with axis of planar symmetry) is applicable throughout the whole transition. The two dimensional diffusion indicates that the structure formed by vortex stirring is compatible with large MLVs. Indeed, low curvatures can be considered as planes and the echo attenuation data follows perfectly the powder distribution curve for 2d water diffusion. It was found before in this system a random mesh phase at low temperatures (below 7°C) [50] and the present data thus suggest the exclusion of a lamellae pierced with holes. In fact, the presence of holes on the bilayers would allow water molecules to move out and across the planes and therefore deviations from the theoretical 2d trend for an ideal lamellar phase would be noticed [51].

## CONCLUSION

The MLVs relaxation to planar lamellae in a non-ionic surfactant system was found to be a discontinuous process (coexistence of both structures) where a kind of nucleation and growth mechanism of planar domains from onion rupture is observed. However, the preparation of MLVs (vortex stirring or controlled shear induced) strongly influences the stability and kinetics of MLVs relaxation as demonstrated by $^2$H-NMR and dynamic rheometry. Due to a higher polydispersity, MLVs prepared by vortex stirring are less stable than the ones prepared under controlled shear rate condition in a rheo-couette. The number density of MLVs (controlled by shear rate) strongly influences the stability. Additionally, the 2 d diffusion (PGSE measurements), found for the vortex stirred sample, indicates of a texture composed by large MLVs. Finally, the self-diffusion coefficients obtained have a remarkable low value (around $6 \cdot 10^{-10}\,\mathrm{m}^2/\mathrm{s}$), which can be compared to the ones obtained for the "ideal lamellar phase" of the AOT/water system.

## REFERENCES

[1] Marlow, S. & Olmsted, P. (2002). *Eur. Phys. J. E*, *8*, 485.

[2] Sierro, P. & Roux, D. (1997). *Phys. Rev. Lett.*, *78*, 1496.

[3] Panizza, P., Colin, A., Coulon, C., & Roux, D. (1998). *Eur. Phys. J. B*, *4*, 65.

[4] Medronho, B., Miguel, M. G., & Olsson, U. (2007). *Langmuir*, *23*, 5270.

[5] Le, T. D., Olsson, U., & Mortensen, K. (2001). *Phys. Chem. Chem. Phys.*, *3*, 1310.

[6] Le, T. D., Olsson, U., Mortensen, K., Zipfel, J., & Richtering, W. (2001). *Langmuir*, *17*, 999.

[7] Diat, O. & Roux, D. (1993). *J. Phys. II*, *3*, 9.

[8] Diat, O., Roux, D., & Nallet, F. (1993). *J. Phys. II*, *2*, 1427.

[9] Zipfel, J., Nettesheim, F., Lindner, P., Le, T. D., Olsson, U., & Richtering, W. (2001). *Europhys. Lett.*, *53*, 335.

[10] Coppola, L., Nicotera, I., & Oliviero, C. (2005). *Applied Rheology*, *4*, 230.

[11] Berghausen, J., Zipfel, J., Lindner, P., & Richtering, W. (1998). *Europhys. Lett.*, *43*, 683.

[12] Coppola, L., Gabriele, D., Nicotera, I., & Oliviero, C. (2004). *Applied Rheology*, *6*, 315.

[13] Mahjoub, H. F., Bourgaux, C., Sergot, P., & Kleman, M. (1998). *Phys. Rev. Lett.*, *81*, 2076.

[14] Mang, J. T., Kumar, S., & Hammouda, B. (1994). *Europhys. Lett.*, *28*, 489.

[15] Mortensen, K. (1996). *J. Phys. Condens. Matter A*, *8*, 103.

[16] Penfold, J., Staples, E., Khan Lodhi, A., Tucker, I., & G. J. T. Tiddy. (1997). *J. Phys. Chem. B.*, *101*, 66.

[17] Pople, J. A., Hamley, I. W., Fairclough, J. P. A., Ryan, A. J., Hill, G., & Prince, C. (1999). *Polymer*, *40*, 5709.

[18] Wunenburger, A. S., Colin, A., Leng, J., Arnéodo, A., & Roux, D. (2001). *Phys. Rev. Lett.*, *86*, 1374.

[19] Léon, A., Bonn, D., Meunier, J., Al-Kahwaji, A., & Kellay, H. (2001). *Phys. Rev. Lett.*, *86*, 938.

[20] Zilman, A. & Granek, R. (1999). *Eur. Phys. J. B II*, *593*, 20.

[21] Le, T. D., Olsson, U., Ortensen, K., Ziphel, J., & Richtering, W. (2001). *Langmuir*, *17*, 999.

[22] Ramos, L., Roux, D., Olmsted, P. D., & Cates, M. E. (2004). *Europhys. Lett.*, *66*, 888, 22.

[23] Courbin, L., Pons, R., Rouch, J., & Panizza, P. (2003). *Europhys. Lett.*, *61*, 275, 23.

[24] Courbin, L., Delville, J. P., Rouch, J., & Panizza, P. (2002). *Phys. Rev. Lett.*, *89*, 148305.

[25] Schmidt, G., Muller, S., Schmidt, C., & Richtering, W. (1999). *Rheol. Acta*, *38*, 486.

[26] Golubovic, L. (1994). *Phys. Rev. E*, *50*, R2419.

[27] Oliviero, C., Coppola, L., Gianferri, R., Nicotera, I., & Olsson, U. (2003). *Colloids and Surfaces A: Physicochem. Eng. Aspects*, *228*, 85.

[28] Aurnhammer, G., Brand, H., & Pleiner, H. (2002). *Phys. Rev. E*, *66*, 0061707.

[29] Zilman, A. & Granek, R. (1999). *Eur. Phys. J. B*, *11*, 593.

[30] Blanc, C., Meyer, C., Asnacios, S., Kleman, M., Lelidis, I., & Marin, J. (2005). *Philosophical Magazine letters*, *85*, 641.

[31] Dhez, O., Nallet, F., & Diat, O. (2001). *Europhys. Lett.*, *55*, 821.

[32] Kleman, M. (1989). *Rep. Prog. Phys.*, *52*, 555.

[33] Diat, O., Roux, D., & Nallet, F. (1993). *J. Phys. IV*, *3*, 193.

[34] Partal, P., Kowalski, A. J., Machin, D., Kiratzis, N., Berni, G., & Lawrence, C. J. (2001). *Langmuir*, *17*, 1331.

[35] Ronemus, A. D., Vold, R. L., & Vold, R. R. (1986). *J. Magn. Reson.*, *70*, 416.

[36] Dimitrova, G. T., Tadros, T. F., Luckham, P. F., & Kipps, M. R. (1996). *Langmuir*, *12*, 315.

[37] Mitchell, D. J., Tiddy, G. J. T., Waring, L., Bostock, T., & Mcdonald, M. P. (1983). *J. Chem. Soc. Faraday Trans. I*, *79*, 975.

[38] Rendall, K. & Tiddy, G. J. T. (1984). *J. Chem. Soc. Faraday Trans.*, *80*, 3339.

[39] Müller, S., Börschig, C., Gronski, W., & Schmidt, C. (1999). *Langmuir*, *15*, 7558.

[40] Pake, G. E. (1948). *J. Chem. Phys.*, *16*, 327.

[41] Gotter, M., Strey, R., Olsson, U., & Wennerstrom, H. (2005). *Faraday Discuss.*, *129*, 327.

[42] Lukaschek, M., Muller, S., Hansenhindl, A., Grabowski, D. A., & Schmidt, C. (1996). *Colloid. Polym. Sci.*, *274*, 1.

[43] Stilbs, P. (1987). *Prog. NMR Spetrosc.*, *18*, 1.

[44] Stejskal, E. O. (1965). *J. Chem. Phys.*, *43*, 3597.

[45] Callaghan, P. T. (1984). *Aust. J. Phys.*, *37*, 359.

[46] Celebre, G., Coppola, L., Ranieri, G. A., & Terenzi, M. (1994). *Mol. Cryst. Liq. Cryst.*, *238*, 117.

[47] Coppola, L., Gianferri, R., Nicotera, I., & Oliviero, C. (2003). *Mol.Cryst. Liq. Cryst.*, *398*, 157.

[48] Ferry, J. D. (1980). in *Viscoelastic Properties of Polymers*, 3rd. ed. Wiley: New York.

[49] Kleinschmidt, F. (2005). *Doctoral Dissertation, Faculty of Chemistry, Pharmacy and Geosciences*, Albert Ludwig University: Freiburg.

[50] Medronho, B., Miguel, M. G., & Olsson, U. (2007). *Langmuir*, *23*, 5270.

[51] Coppola, L., Gianferri, R., Nicotera, I., & Oliviero, C. (2003). *Mol. Cryst. Liq. Cryst.*, *398*, 157.